A stable, power scaling, graphene-mode-locked all-fiber oscillator

D. Popa,[1, a)] Z. Jiang,[1] G. E. Bonacchini,[1] Z. Zhao,[1] L. Lombardi,[1] F. Torrisi,[1] A. K. Ott,[1] E. Lidorikis,[2] and A. C. Ferrari[1]

[1)] *Cambridge Graphene Centre, University of Cambridge, Cambridge CB3 0FA, UK*

[2)] *Department of Materials Science and Engineering, University of Ioannina, Ioannina 45110, Greece*

We report power tunability in a fiber laser mode-locked with a solution-processed filtered graphene film on a fiber connector. ∼370fs pulses are generated with output power continuously tunable from∼4 up to∼52mW. This is a simple, low-cost, compact portable all-fiber ultrafast source for applications requiring environmentally stable, portable sources, such as imaging.

Optical pulses generated by mode-locked lasers are increasingly used in a variety of applications, supporting developments in many scientific, commercial and industrial areas[1,2]. The success of lasers in this field, is partly fueled by their ability to generate pulses matching various application needs[1–5]. In medicine, depending on the particular application (e.g. surgery[2] or imaging[4,5]), optical pulses operating at specific wavelengths are needed to fit the absorption and scattering profile of a tissue[6]. E.g. for tissue imaging[4,5], wavelengths in the ∼1-1.5μm range minimize photodamage and maximize penetration depth[1–5]. Similarly, the pulse duration specifies the type of laser-tissue interaction that may occur[1–5], while the pulse repetition rate controls the interaction speed[1–5]. Ultimately, the optical power delivered to the sample needs to balance the desired laser-tissue interaction with any non-desired, e.g. photodamage, effects[1–3]. E.g., in nonlinear microscopy lasers with high, ∼kW level, peak powers are used to generate nonlinear signals of interest while keeping the average power at a few 10s mWs, i.e. below the sample photodamage threshold[1,3,5]. An important goal is to enable real-time imaging in the operating room or outpatient setting[3,4], requiring compact and stable light sources[1,3,4]. Commercially available solid-state lasers, such as titanium-sapphire (Ti:Sa) lasers pumping optical parametric oscillators (OPOs), can provide a 700-4000 nm tuning range with several hundred mW average power[7]. However, both are complex and expensive systems, relying on bulk optics[1]. This has driven a research effort to find novel approaches, not only capable of producing short pulses, but also cheaper, simpler, broadband, and stable. Fiber lasers are attractive platforms for short pulse generation due to their simple and compact designs[8], efficient heat dissipation[2], and alignment-free operation[1,2]. These characteristics, combined with advances in glass technology[9,10] and nonlinear optics[11], resulted in systems working from the visible to the mid-infrared[9]. In fiber oscillators, ultrashort pulses can be obtained by passive mode-locking. This typically requires the aid of a non-linear component called a saturable absorber (SA)[1,8]. Graphene[12,13] and carbon nanotubes (CNTs)[12,14–18] have emerged as promising SAs for ultrafast lasers[13–30]. In CNTs, broadband operation is achieved by using a distribution of tube diameters[17,20], while this is an intrinsic property of graphene[32]. This, along with the ultrafast recovery time[33], low saturation fluence[13,31], environmental stability[29], and ease of fabrication[34] and integration[35], makes graphene an excellent broadband SA[32]. Consequently, mode-locked lasers using graphene SAs (GSAs) have been demonstrated from∼800nm[36] to ∼970nm[37], ∼1μm[38], ∼1.5μm[31], ∼2μm[39], and ∼2,4μm[40] up to ∼2,8μm[41]. Various approaches have been used to prepare GSAs for mode-locked fiber oscillators with output powers greater than 10mW, as required for laser imaging[1,3]. E.g., dispersions produced by liquid phase exfoliation (LPE) of graphite[42], were used to generate∼60mW at 1.1μm[43], and∼15mW at 1.5μm[44]. Films grown by chemical vapor deposition (CVD) with 1 layer[45], 1-2 layers[46], and several layers[47,48], were used to generate∼115mW at 2μm[45], ∼15mW at 1.5μm[46],∼44mW at 2μm[47], and∼174mW at 1.5μm[48]. Graphene oxide (GO) was also used as an SA, to generate∼148mW at 1μm[49], and∼80mW at 1.5μm[50]. However, GO is an insulating with many defects and gap states[51], and may not offer the wideband tunability of GSAs. Flakes grown by CVD require high substrate temperatures[35], followed by transfer to the target substrate[35]. LPE has the advantage of scalability, room temperature processing and high yield, and does not require any substrate[35]. Dispersions produced by LPE can easily be integrated into various systems[34,35].

Here we use a LPE polymer-free graphene film coated on a fiber based connector as SA. Based on this, we demonstrate mode-locking of an all-fiber laser, achieving stable pulses with duration∼370fs over a continuous output power tuning range from∼3.5 to ∼52mW. This enables simple and robust light sources for applications such as laser imaging[3], with adjustable output power and no need of amplification stages.

The GSA is prepared and characterized as described in Ref.38. Graphite (Sigma Aldrich) is exfoliated via ultrasonic treatment in a solution of deionised water and sodium cholate (0.9wt%)[13,52], followed by ultracentrifugation at 10000rpm for 1 hour. The resulting 70% top dispersion is then filtered in vacuum through a nitrocel-

[a)] Electronic mail: dp387@cam.ac.uk

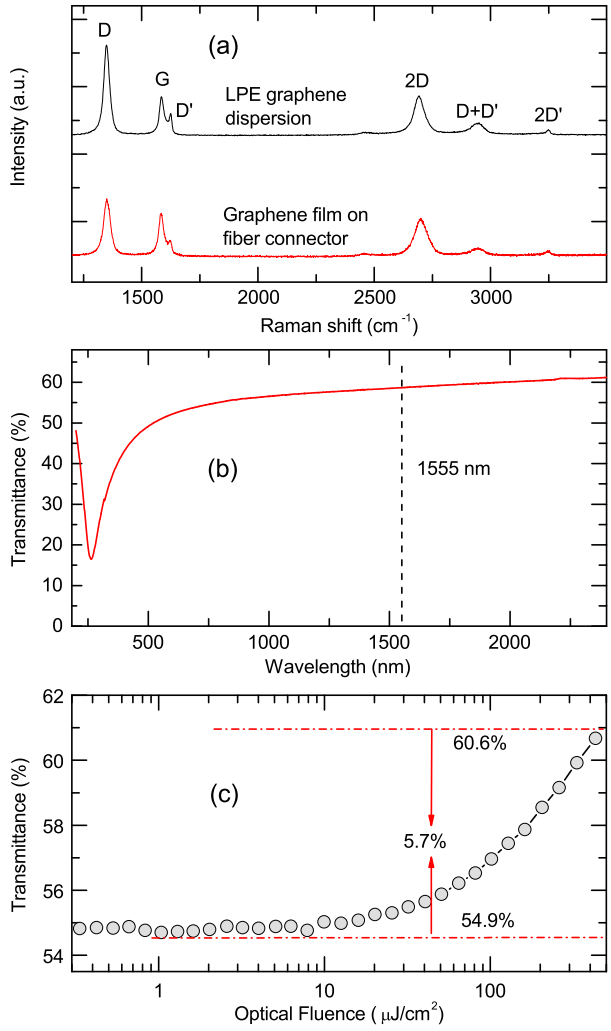

FIG. 1. Raman characterization, linear and non-linear response. (a) Raman spectra of film and LPE graphene dispersion. (b) Linear transmittance of film, showing featureless behavior from ∼500 to ∼2400nm. The dip at∼266nm is due to the van Hove singularity in the graphene density of states[58]. The laser operating wavelength is marked. (c) Non-linear transmittance at the laser operating wavelength.

lulose membrane (Millipore 100nm pore-size filter). This blocks the flakes, while allowing water to pass through, resulting in a film on the top of the membrane. The film is then placed onto the tip of a fiber connector for physical contact (FC/PC), to be used in the laser, and on a quartz plate, for optical characterization, by applying pressure and heat (∼90°C, to improve adhesion) for 1 hour, followed by dissolution of the filter in acetone.

To monitor the film quality after filtration, we characterize it by Raman Spectroscopy at 457, 514 and 633nm, using a Renishaw InVia micro-Raman spectrometer. Fig.1(a) plots a tipycal Raman spectrum (black curve) of representative flakes of the LPE dispersion on Si/SiO_2[38]. Besides the G and 2D peaks, presents significant D and D' bands as well as their combination mode

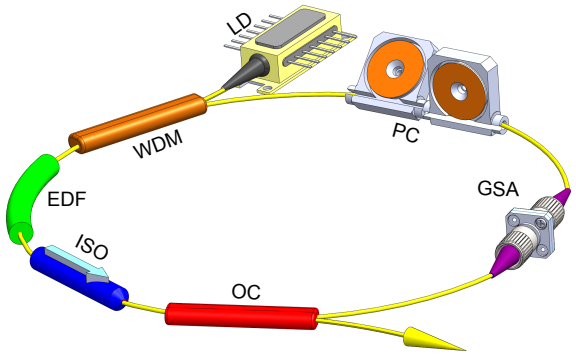

FIG. 2. Laser schematic. LD: Laser diode; WDM: Wavelength division multiplexer; EDF: Erbium doped fiber; ISO: Isolator; OC: Optical coupler; PC: Polarization controller.

D+D' at ∼2950cm^{-1}[53]. The D and D' peaks are assigned to the sub-micrometer edges of our flakes[54], rather than to disorder within the flakes[54], also supported by low Disp(G) ∼0.05cm^{-1}/nm[55], much lower than in disordered carbons[56]. Similarly to LPE, Fig.1(a) plots the Raman spectrum (red curve) of the film on the FC/PC tip, with Disp(G) ∼0.02cm^{-1}/nm. The full width at half maximum FWHM(2D) (peak at ∼76 cm^{-1}) is ∼17 cm^{-1} larger that of the LPE dispersion. However, the 2D peak is still Lorentzian, thus, even if the flakes are multi-layers, they are electronically decoupled and, to a first approximation, behave as a collection of single layers[57]. We conclude that the filtration does not affect the structure of the flakes in our film.

Fig.1(b) plots the GSA transmittance. Except for the peak at∼266 nm, a signature of the van Hove singularity in the graphene density of states[58], the spectrum has a featureless linear transmission from ∼500 to ∼2400nm. The transmittance and absorption at 1555 nm (the laser wavelength) are∼59% and ∼30% respectively. Ref.38 used the transfer matrix formalism[59] to estimate the number of graphene layers (N). We apply this formalism and calculate, as a function of N, the absorption of our GSA. In this model, the film is approximated as a multilayered graphene on a quartz substrate. The overall absorption is calculated by evaluating the contributions of multiple reflections. By comparing our calculations with the data at 1555 nm we estimate that a 30% absorption translates to N∼35-40 layers. The nonlinear optical transmittance is measured with an OPO (Coherent, Chameleon) delivering∼570fs pulses with 4MHz repetition rate at 1555nm. The optical transmittance is determined by monitoring the input and output power, Fig.1(c). The transmittance increases from∼54.9% to ∼60.6%, a change of ∼5.7%, preferred for mode-locking of fiber lasers[60], that typically operate with higher gain and cavity losses[8] than their solid-state counterparts[61].

For our oscillator, we design a dispersion-managed soliton laser, able to support higher pulse energies than soliton lasers[19,22,31], as shown in Fig.2, with a total

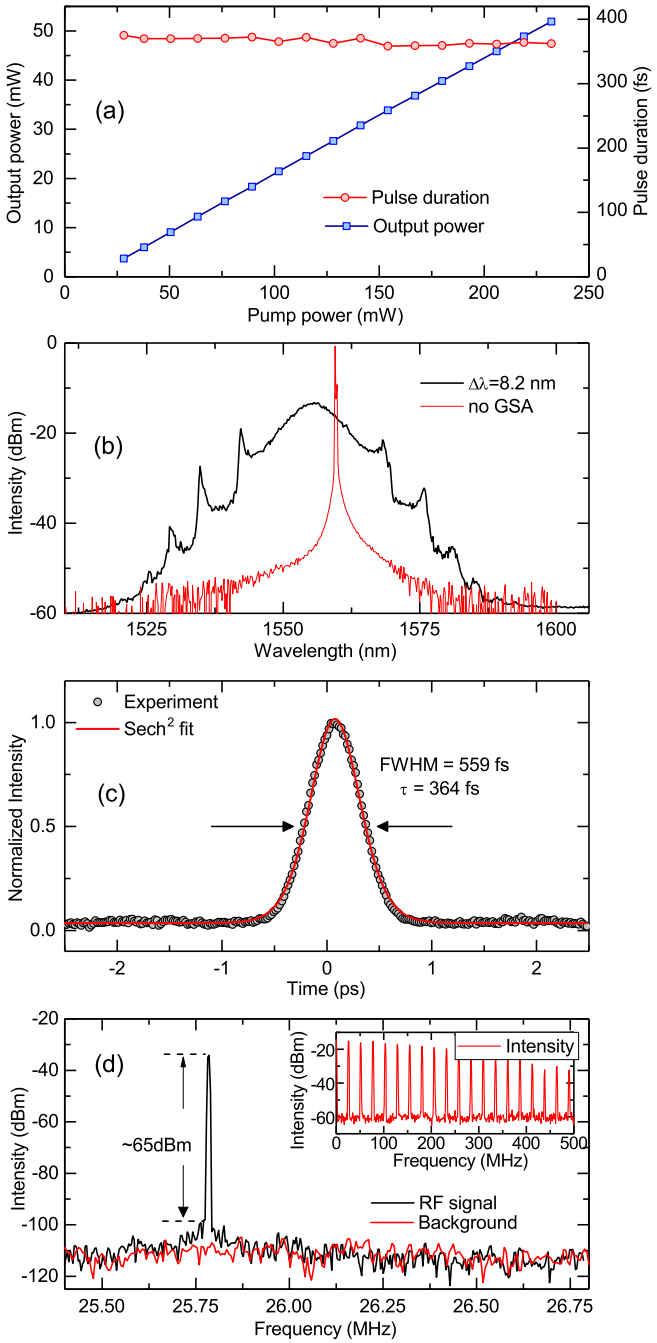

FIG. 3. Mode-locking results. (a) Scaling of output power and variation of pulse duration with pump power, and a set of laser measurements recorded at maximum output power, showing (b) Optical spectrum with∼1555nm center wavelength and∼8.2nm spectral width, with the red line showing CW operation when the GSA is removed, (c) Autocorrelation trace with pulse duration∼364fs, and (d) first harmonic of the RF spectrum with∼65dBm peak to pedestal extinction ratio. Inset: RF spectrum at maximum output power with 500MHz span.

cavity length ∼8m. We use a ∼2.3m erbium doped fiber (EDF), with a second-order dispersion coefficient $\beta^{(2)} \sim 22ps^2/km$ as gain medium. The EDF is pumped by a 980 nm continuous wave (CW) laser diode (LD) through a fused wavelength division multiplexer (WDM). The rest of the cavity is formed from two lengths of standard single mode fiber (SMF): ∼5.3m of SMF-28 with $\beta^{(2)} \sim -22ps^2/km$, and ∼0.4m of Flexcore-1060 with $\beta^{(2)} \sim -7ps^2/km$. This gives a net intracavity second-order dispersion ∼ -0.07ps^2, typical of dispersion-managed soliton lasers[19,22,31]. Unidirectional propagation is ensured by an optical isolator (ISO). A polarization controller (PC) is used for mode-locking optimization and stabilization. In order to reduce the effects that high power injected in the fiber could have on graphene[62] and its stability, the output of the laser is provided by the 70% port of a 70/30 output coupler (OC). The total cavity length is∼8m. Mode-locking starts at∼28mW pump power, with P_{out} ∼3.7mW output power. The average P_{out} then scales up linearly with pump power as in Fig.3(a), with a maximum P_{out} ∼52mW at 232mW pump. For this power range we measure a maximum∼367±8fs variation in the pulse duration, as shown in Fig.3(a). The pulse optical spectrum plotted in Fig.3(b), with $\Delta\lambda$=8.2nm spectral width, exhibits sidebands related to a periodic disturbance of soliton pulses in the laser resonator[1,2], as expected for soliton operation in fiber lasers[1]. Removing the GSA results in CW operation of the laser [Fig.3(b) red line]. The corresponding intensity autocorrelation trace, pedestal free, is shown in Fig.3(c), with $\Delta\tau$=364fs pulse duration, as determined by fitting a $sech^2$ profile to the pulse, as expected for soliton-like mode-locking[63]. This gives a time bandwidth product $\Delta\nu\Delta\tau$=0.37, close to the expected transform-limit 0.315[64]. The radio frequency (RF) spectrum of the pulse train, measured with a photodetector connected to an RF spectrum analyzer, is reported in Fig.3(d), for the first harmonic, 25.8MHz, and up to 500MHz. The fundamental repetition rate matches the cavity length, thus confirming single pulse operation. A signal-to-noise ratio ∼65dB indicates pulse stability up to the maximum output power. For P_{out}=52mW, the corresponding pulse energy is E_c=2nJ and the peak power P_{peak}=5kW. For higher P_{out}, i.e. increasing the pump power over 232mW, pulse breaking is observed, which can be attributed to optical non-linearities in the fiber arising from high intra-cavity peak intensities[63]. Use of photonic crystal fibers with tailored nonlinearities[10] could enable higher output powers which, combined with the broadband nature of graphene[32], could, in principle, extend our approach at other wavelengths.

Compared to Ti:Sa and OPOs, our all-fiber design, exploiting a GSA, is simpler to assemble, needing no critical alignment. A graphene-based all-fiber setup capable of P_{out} ∼15mW pulses at ∼1560nm was reported in Ref.65. However, the use of a multilayer CVD graphene/poly methyl methacrylate structure complicates the fabrication process[65]. Ref. 43 used a LPE based GSA to generate P_{out} ∼60mW at 1180nm. Despite the higher P_{out}, the pulses were∼200ns long, with lower P_{peak} <1W[43],

than the ∼5kW in our laser.

In conclusion, we demonstrated a mode-locked all-fiber laser with output power adjustable from 3.7 to 52mW, using a GF as SA. The maximum pulse energy is E_c=2nJ corresponding to a P_{peak} ∼5kW, making it attractive for applications such as laser imaging.

We acknowledge funding from the EU Graphene Flagship (no. 604391), ERC Grants Hetero2D and HiGraphink, EPSRC Grants EP/K01711X/1, EP/K017144/1, Emmanuel College, Cambridge, and Trinity College, the Isaac Newton Trust.

[1] M. E. Fermann, A. Galvanauskas and G. Sucha, *Ultrafast Lasers: Technology and Applications*, (CRC Press, 2002).
[2] F. Dausinger, F. Lichtner, and H. Lubatschowski, Top. Appl. Phys. **96**, 326 (2004).
[3] C. Krafft, I. W. Schie, T. Meyer, M. Schmitt, J. Popp, Chem. Soc. Rev. **45**, 1819 (2016).
[4] N. Vogler, S. Heuke, T. W. Bocklitz, M. Schmitt and J. Popp, Annu. Rev. Anal. Chem. **8**, 359 (2015).
[5] C. L. Evans and X. S. Xie, Annu. Rev. Anal. Chem. **1**, 883 (2008).
[6] W. F. Cheong, S. A. Prahl and A. J. Welch, IEEE J. Quantum Electron. **26**, 2166 (1990).
[7] http://www.coherent.com/download/6416/Chameleon-Ultra-Family-Data-Sheet.pdf
[8] M. E. Fermann, and I. Hartl, Nat. Photonics **7**, 868 (2013).
[9] M. J. F. Digonnet, *Rare earth doped fiber lasers and amplifiers*, (Marcel Dekker, NY, USA, 1993).
[10] P. Russell, Science **299**, 358 (2003).
[11] J. M. Dudley, J. R. Taylor, Nat. Photonics **3**, 85 (2009).
[12] T. Hasan, Z. Sun, F. Wang, F. Bonaccorso, P. H. Tan, A. G. Rozhin, and A. C. Ferrari, Adv. Mater. **21**, 3874 (2009).
[13] Z. Sun, T. Hasan, F. Torrisi, D. Popa, G. Privitera, F. Wang, F. Bonaccorso, D. M. Basko, A. C. Ferrari, ACS Nano, **4**, 803 (2010).
[14] S. Y. Set, H. Yaguchi, Y. Tanaka, and M. Jablonski, IEEE J. Sel. Top. Quantum Electron. **10**, 137 (2004).
[15] S. Y. Set, H. Yaguchi, Y. Tanaka and M. Jablonski, J. Lightwave Technol. **22**, 51 (2004).
[16] S. Yamashita, Y. Inoue, S. Maruyama, Y. Murakami, H. Yaguchi, M. Jablonski and S. Y. Set, Opt. Lett. **29**, 1581 (2004).
[17] F. Wang, A. G. Rozhin, V. Scardaci, Z. Sun, F. Hennrich, I. H. White, W. I. Milne, and A. C. Ferrari, Nat. Nano. **3**, 738 (2008).
[18] V. Scardaci, Z. P. Sun, F. Wang, A. G. Rozhin, T. Hasan, F. Hennrich, I. H. White, W. I. Milne, and A. C. Ferrari, Adv. Mater. **20**, 4040 (2008).
[19] D. Popa, Z. Sun, T. Hasan, W. Cho, F.Wang, F. Torrisi, and A. Ferrari, Appl. Phys. Lett. **101**, 153107 (2012).
[20] R. Going, D. Popa, F. Torrisi, Z. Sun, T. Hasan, F. Wang, and A. C. Ferrari, Physica E, **44**, 1078 (2012).
[21] Z. Zhang, D. Popa, V. J. Wittwer, S. Milana, T. Hasan, Z. Jiang, A. C. Ferrari, F. . Ilday, Appl. Phys. Lett. **107**, 241107 (2015).
[22] D. G. Purdie, D. Popa, V. J. Wittwer, Z. Jiang, G. Bonacchini, F. Torrisi, S. Milana, E. Lidorikis, A. C. Ferrari, Appl. Phys. Lett. **106**, 253101 (2015).
[23] Y. Ren, G. Brown, R. Mary, G. Demetriou, D. Popa, F. Torrisi, A. C. Ferrari, F. Chen, A. K. Kar, IEEE J. Sel. Top. Quantum Electron. **21**, 395 (2015).
[24] R. Mary, G. Brown, S. J. Beecher, R. R. Thomson, D. Popa, Z. Sun, F. Torrisi, T. Hasan, S. Milana, F. Bonaccorso, A. C. Ferrari, A. K. Kar, Appl. Phys. Lett. **103**, 221117 (2013).
[25] C. E. S. Castellani, E. J. R. Kelleher, D. Popa, T. Hasan, Z. Sun, A. C. Ferrari, S. V. Popov, J. R. Taylor, Laser Phys. Lett. **10**, 015101 (2013).
[26] M. Zhang, E. J. R. Kelleher, T. H. Runcorn, V. M. Mashinsky, O. I. Medvedkov, E. M. Dianov, D. Popa, S. Milana, T. Hasan, Z. Sun, F. Bonaccorso, Z. Jiang, E. Flahaut, B. H. Chapman, A. C. Ferrari, S. V. Popov, J. R. Taylor, Opt. Express **21**, 23261 (2013).
[27] R. I. Woodward, E. J. R. Kelleher, D. Popa, T. Hasan, F. Bonaccorso, A. C. Ferrari, S. V. Popov, and J. R. Taylor, IEEE Photonic Tech. L. **26**, 1672 (2014).
[28] D. Popa, Z. Sun, T. Hasan, F. Torrisi, F. Wang, and A. C. Ferrari, Appl. Phys. Lett. **98**, 073106 (2011).
[29] F. Torrisi, D. Popa, S. Milana, Z. Jiang, T. Hasan, E. Lidorikis, and A. C. Ferrari, Adv. Opt. Mat. **4**, 1088 (2016).
[30] Z. Sun, D. Popa, T. Hasan, F. Torrisi, F. Wang, E. J. R. Kelleher, J. C. Travers, V. Nicolosi, A. C. Ferrari, Nano Res. **3**, 653 (2010).
[31] D. Popa, Z. Sun, F. Torrisi, T. Hasan, F. Wang, and A. C. Ferrari, Appl. Phys. Lett. **97**, 203106 (2010).
[32] F. Bonaccorso, Z. Sun, T. Hasan, and A. C. Ferrari, Nat. Photonics **4**, 611 (2010).
[33] D. Brida, A. Tomadin, C. Manzoni, Y. J. Kim, A. Lombardo, S. Milana, R. R. Nair, K. S. Novoselov, A. C. Ferrari, G. Cerullo, M. Polini, Nature Commun. **4**, 1987 (2013).
[34] A. C. Ferrari, F. Bonaccorso, V. Falko, K. S. Novoselov, S.Roche, P. Boggild, S. Borini, F. Koppens, V. Palermo, N. Pugno, et al. Nanoscale **7**, 4598 (2015).
[35] F. Bonaccorso, A. Lombardo, T. Hasan, Z. P. Sun, L. Colombo, and A. C. Ferrari, Materials Today, **15**, 564 (2012).
[36] I. H. Baek, H. W. Lee, S. Bae, B. H. Hong, Y. H. Ahn, D.-I. Yeom and F. Rotermund, Appl. Phys. Express **5**, 032701 (2012).
[37] C. A. Zaugg, Z. Sun, V. J. Wittwer, D. Popa, S. Milana, T. S. Kulmala, R. S. Sundaram, M. Mangold, O. D. Sieber, M. Golling, Y. Lee, J. H. Ahn, A. C. Ferrari, and U. Keller, Opt. Express **21**, 31548 (2013).
[38] R. Mary, S. J. Beecher, G. Brown, F. Torrisi, S. Milana, D.Popa, T. Hasan, Z. Sun, E. Lidorikis, S. Ohara, A. C. Ferrari, and A. K. Kar, Opt. Express **21**, 7943 (2013).
[39] M. Zhang, E. J. R. Kelleher, F. Torrisi, Z. Sun, T. Hasan, D. Popa, F. Wang, A. C. Ferrari, S. V. Popov, and J. R. Taylor, Opt. Express. **20** 25077 (2012).
[40] M. N. Cizmeciyan, J. W. Kim, S. Bae, B. H. Hong, F. Rotermund and A. Sennaroglu, Opt. Lett. **38**, 341 (2013).
[41] G. Zhu, X. Zhu, F. Wang, S. Xu, Y. Li, X. Guo, K. Balakrishnan, R. A. Norwood, N. Peyghambarian, IEEE Photonic Tech. L. **28**, 7 (2016).
[42] Y. Hernandez, V. Nicolosi, M. Lotya, F. M. Blighe, Z. Y. Sun, S. De, I. T. McGovern, B. Holland, M. Byrne, Y. K. Gun'ko, J. J. Boland, P. Niraj, G. Duesberg, S. Krishnamurthy, R. Goodhue, J. Hutchison, V. Scardaci, A. C. Ferrari, J. N. Coleman, Nat. Nano. **3**, 563 (2008).
[43] L. Zhang, G. Wang, J. Hu, J. Wang, J. Fan, J. Wang, Y. Feng, IEEE Photonics Journal **4**, 1809 (2012).
[44] Z. Jiang, G. E. Bonacchini, D. Popa, F. Torrisi, A. K. Ott, V. J. Wittwer, D. Purdie, A. C. Ferrari, in CLEO: 2014. (Optical Society of America, San Jose, California, 2014), pp. JTu4A.67.
[45] H. Jeong, S. Y. Choi, M. H. Kim, F. Rotermund, Y.-H. Cha, D.-Y. Jeong, S. B. Lee, K. Lee, D.-I. Yeom, Opt. Express **24**, 14152 (2016).
[46] J. Park, K. Park, D. Spoor, B. Hall, Y.-W. Song, Opt. Express **23**, 7940 (2015).
[47] J. Sotor, M. Pawliszewska, G. Sobon, P. Kaczmarek, A. Przewolka, I. Pasternak, J. Cajzl, P. Peterka, P. Honztko, I. Kak, W. Strupinski, K. Abramski, Opt. Lett. **41**, 2592 (2016).
[48] C. Sun Young, J. Hwanseong, H. Byung Hee, R. Fabian, Y. Dong-Il, Laser Phys. Lett. **11**, 015101 (2014).
[49] Z. Cheng, H. Li, H. Shi, J. Ren, Q.-H. Yang, P. Wang, Opt. Express **23**, 7000 (2015).
[50] S. Y. Choi, D. K. Cho, Y.-W. Song, K. Oh, K. Kim, F. Rotermund, D.-I. Yeom, Opt. Express **20**, 5652 (2012).
[51] C. Mattevi, G. Eda, S. Agnoli, S. Miller, K. A. Mkhoyan, O. Celik, D. Mastrogiovanni, G. Granozzi, E. Garfunkel, M. Chhowalla, Adv. Funct. Mater. **19**, 2577 (2009).
[52] T. Hasan, F. Torrisi, Z. Sun, D. Popa, V. Nicolosi, G. Privitera, F. Bonaccorso, A. C. Ferrari, Phys. Status Solidi B **247**, 2953 (2010).

[53]A. C. Ferrari, J. C. Meyer, V. Scardaci, C. Casiraghi, M. Lazzeri, F. Mauri, S. Piscanec, D. Jiang, K. S. Novoselov, S. Roth, A. K. Geim, Phys. Rev. Lett. **97**, 187401 (2006).
[54]C. Casiraghi, A. Hartschuh, H. Qian, S. Piscanec, C. Georgi, A. Fasoli, K. S. Novoselov, D. M. Basko, and A. C. Ferrari, Nano Lett, **9**, 1433 (2009).
[55]F. Torrisi, T. Hasan, W. Wu, Z. Sun, A. Lombardo, T. S. Kulmala, G.-W. Hsieh, S. Jung, F. Bonaccorso, P. J. Paul, D. Chu, and A. C. Ferrari, ACS Nano **6**, 2992 (2012).
[56]A. C. Ferrari, and J. Robertson, Phys. Rev. B **64**, 075414 (2001).
[57]S. Latil, V.Meunier, L.Henrard, Phys. Rev. B **76**, 201402 (2007).
[58]V. G. Kravets, A. N. Grigorenko, R. R. Nair, P. Blake, S. Anissimova, K. S. Novoselov, A. K. Geim, Phys. Rev. B **81**, 155413 (2010).
[59]M. Born, E. Wolf, *Principles of Optics: Electromagnetic Theory of Propagation, Interference and Diffraction of Light* (Cambridge University Press, 1999).
[60]A. Cabasse, G. Martel, J. L. Oudar, Opt. Express **17**, 9537 (2009).
[61]W. Koechner, *Solid-State Laser Engineering* (Springer, 1999).
[62]M. Currie, J. D. Caldwell, F. J. Bezares, J. Robinson, T. Anderson, H. Chun and M. Tadjer, Appl. Phys. Lett. **99**, 211909 (2011).
[63]G. P. Agrawal, *Applications of Nonlinear Fiber Optics* (Academic Press, London, (2001).
[64]U. Keller, in *Progress in Optics* **46**, 1 (Elsevier, 2004).
[65]J. Tarka, J. Boguslawski, G. Sobon, I. Pasternak, A. Przewloka, W. Strupinski, J. Sotor, K. M. Abramski, IEEE J. Sel. Top. Quantum Electron. **23**, 1 (2017).

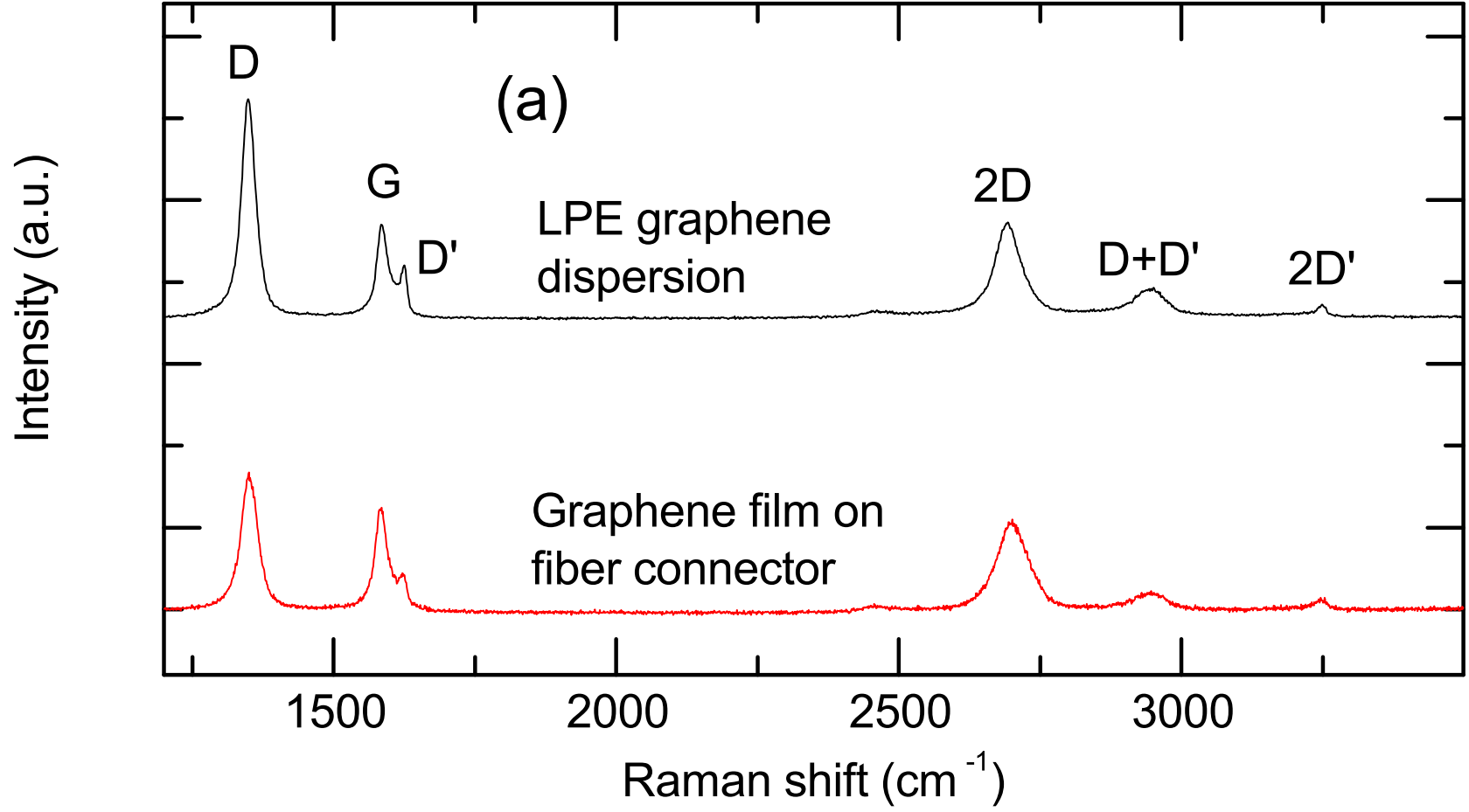
(a)
D
G
D'
2D
D+D'
2D'
LPE graphene
dispersion
Graphene film on
fiber connector
Intensity (a.u.)
1500
2000
2500
3000
Raman shift (cm -1)

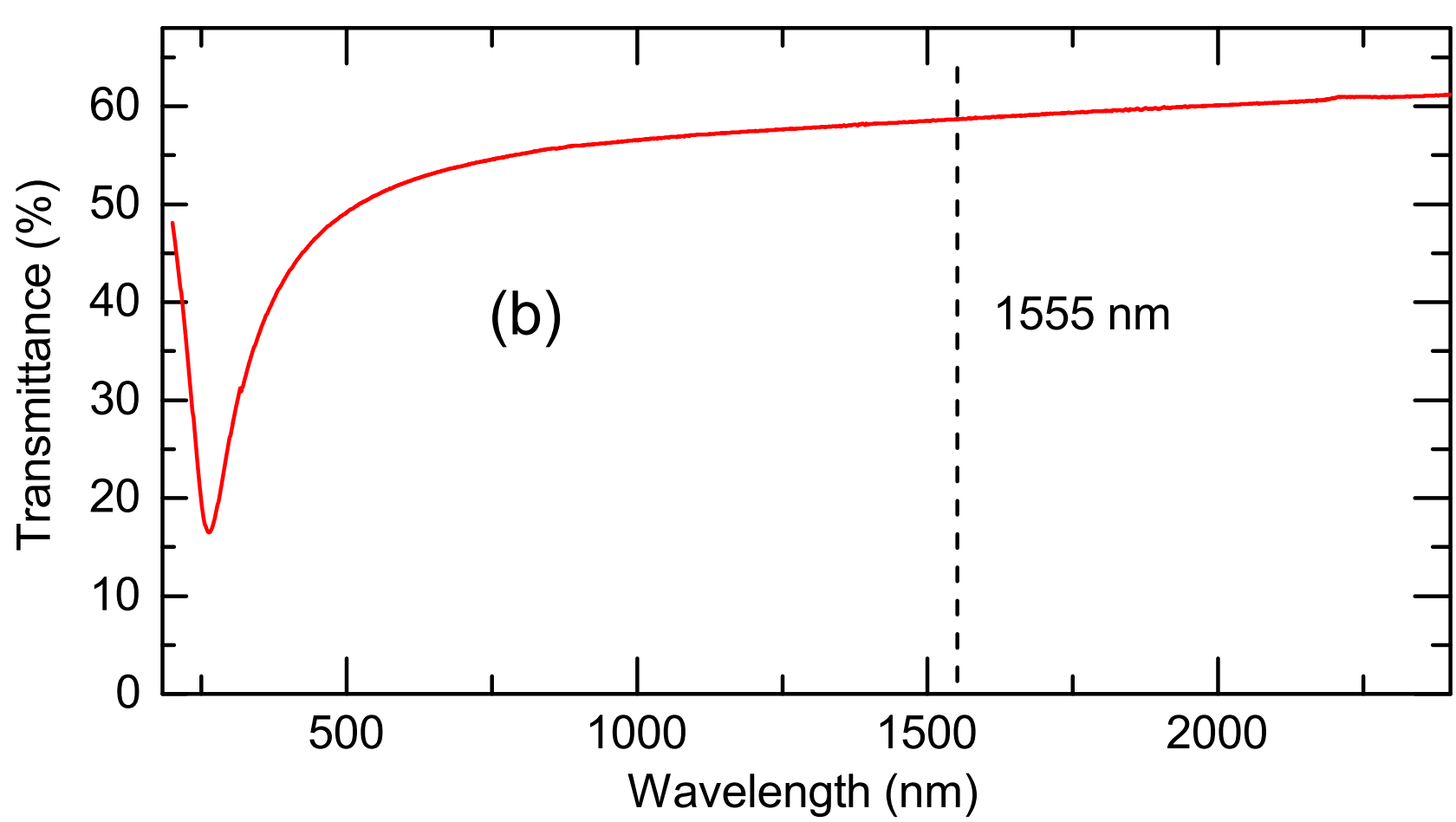
(b)
1555 nm
Transmittance (%)
60
50
40
30
20
10
0
500
1000
1500
2000
Wavelength (nm)

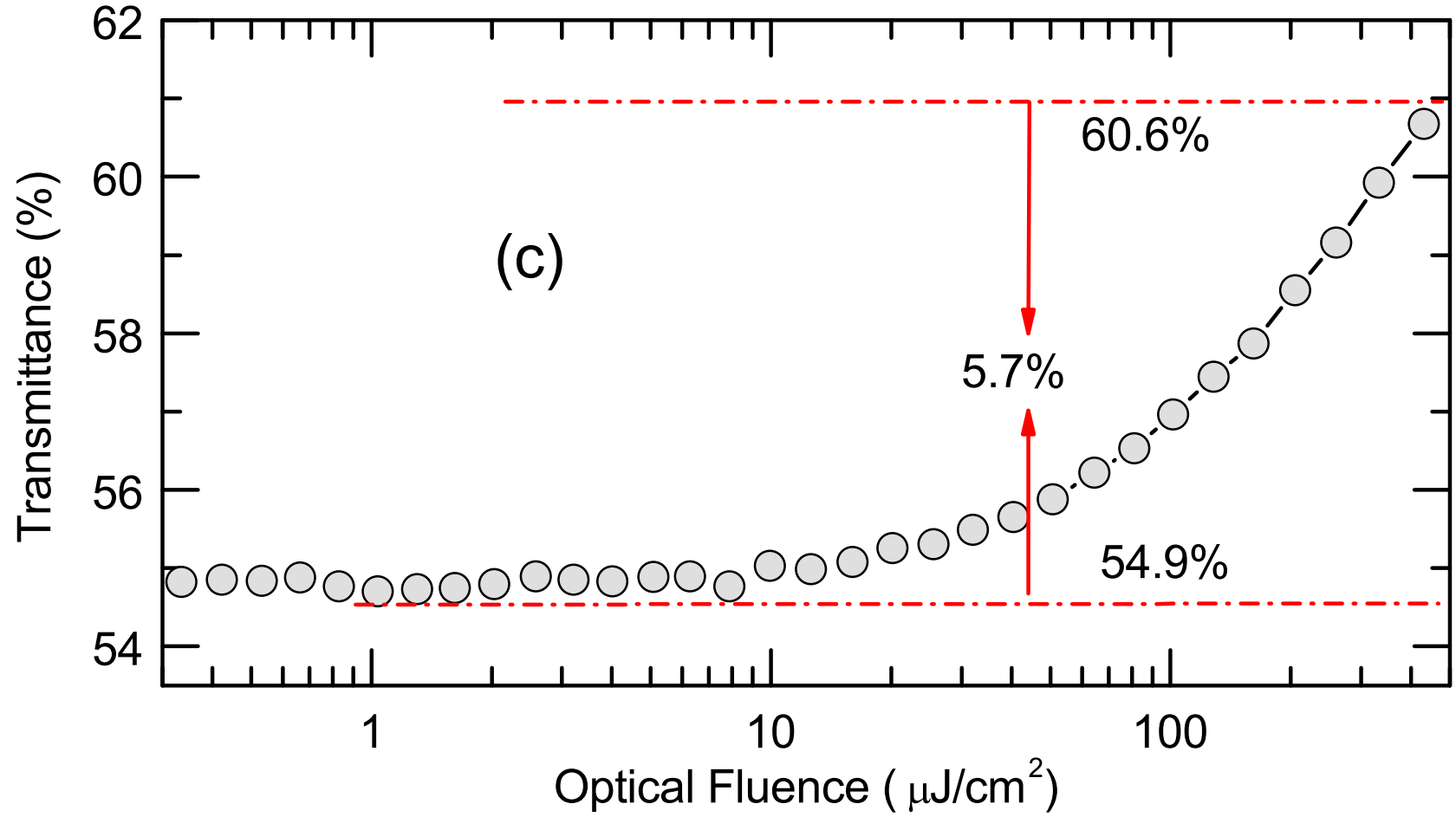
(c)
60.6%
5.7%
54.9%
Transmittance (%)
62
60
58
56
54
1
10
100
Optical Fluence (μJ/cm2)

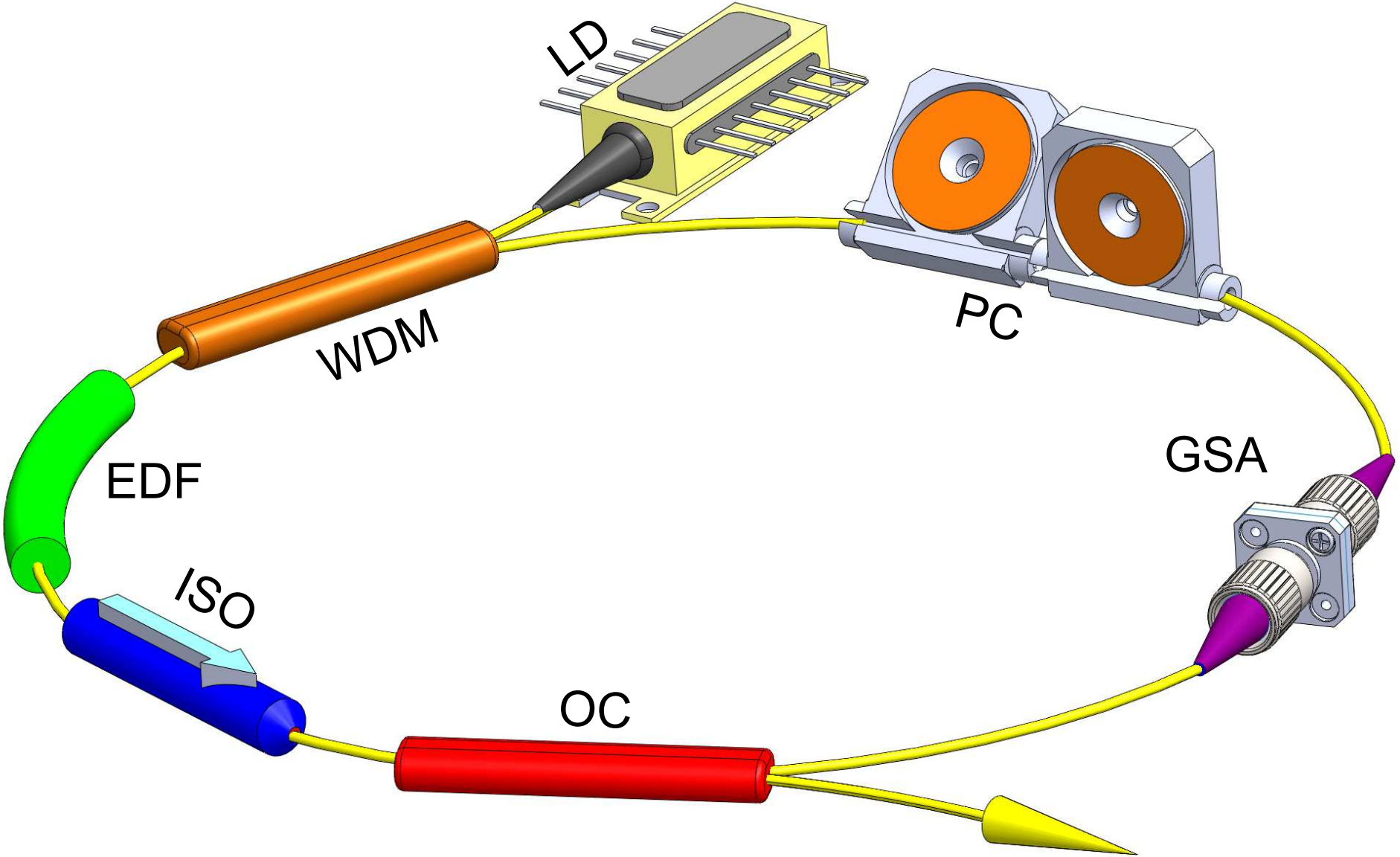
LD
PC
WDM
EDF
GSA
ISO
OC

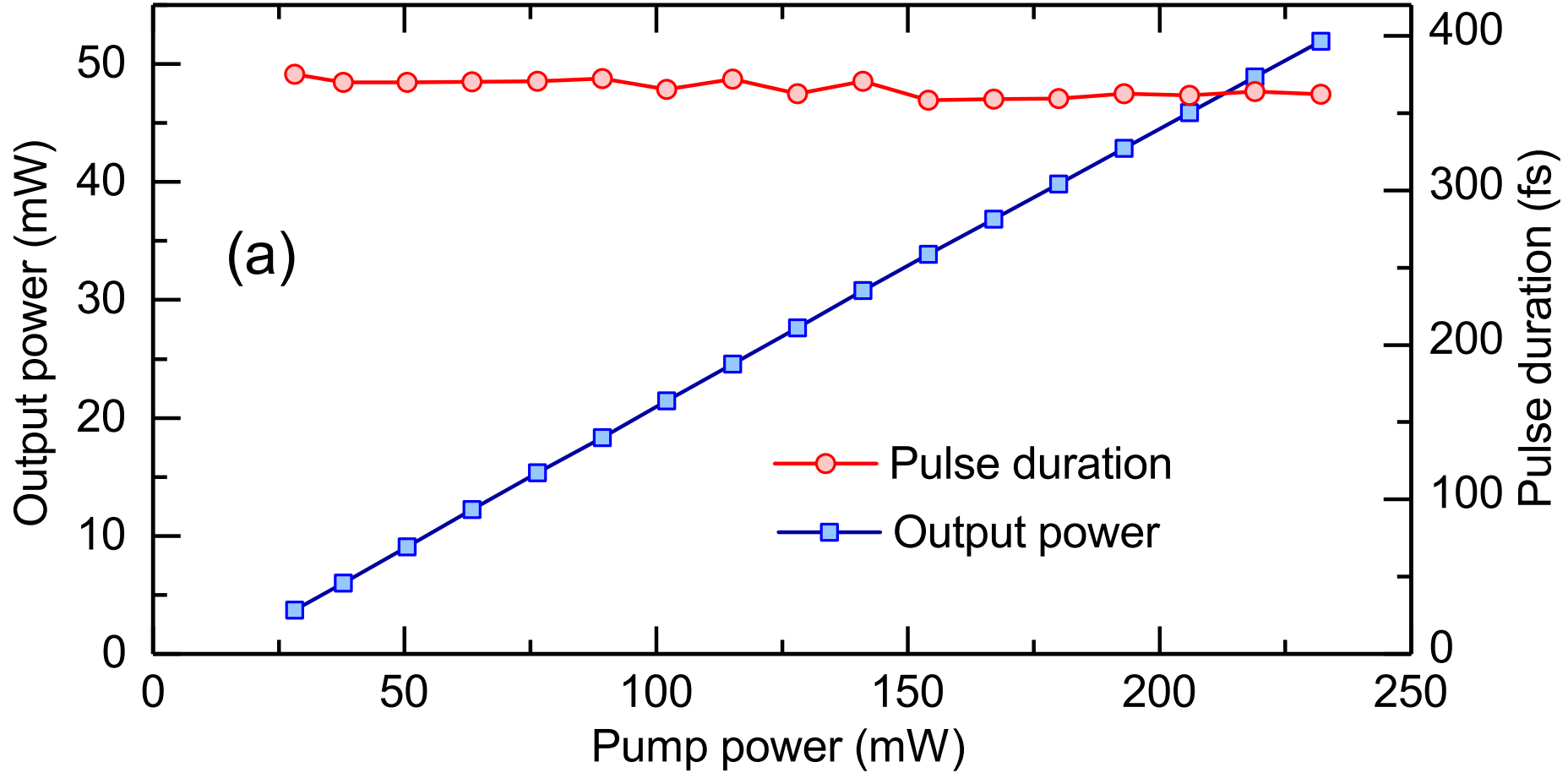
(a)
Output power (mW)
Pulse duration (fs)
Pump power (mW)
Pulse duration
Output power
0
10
20
30
40
50
0
100
200
300
400
0
50
100
150
200
250

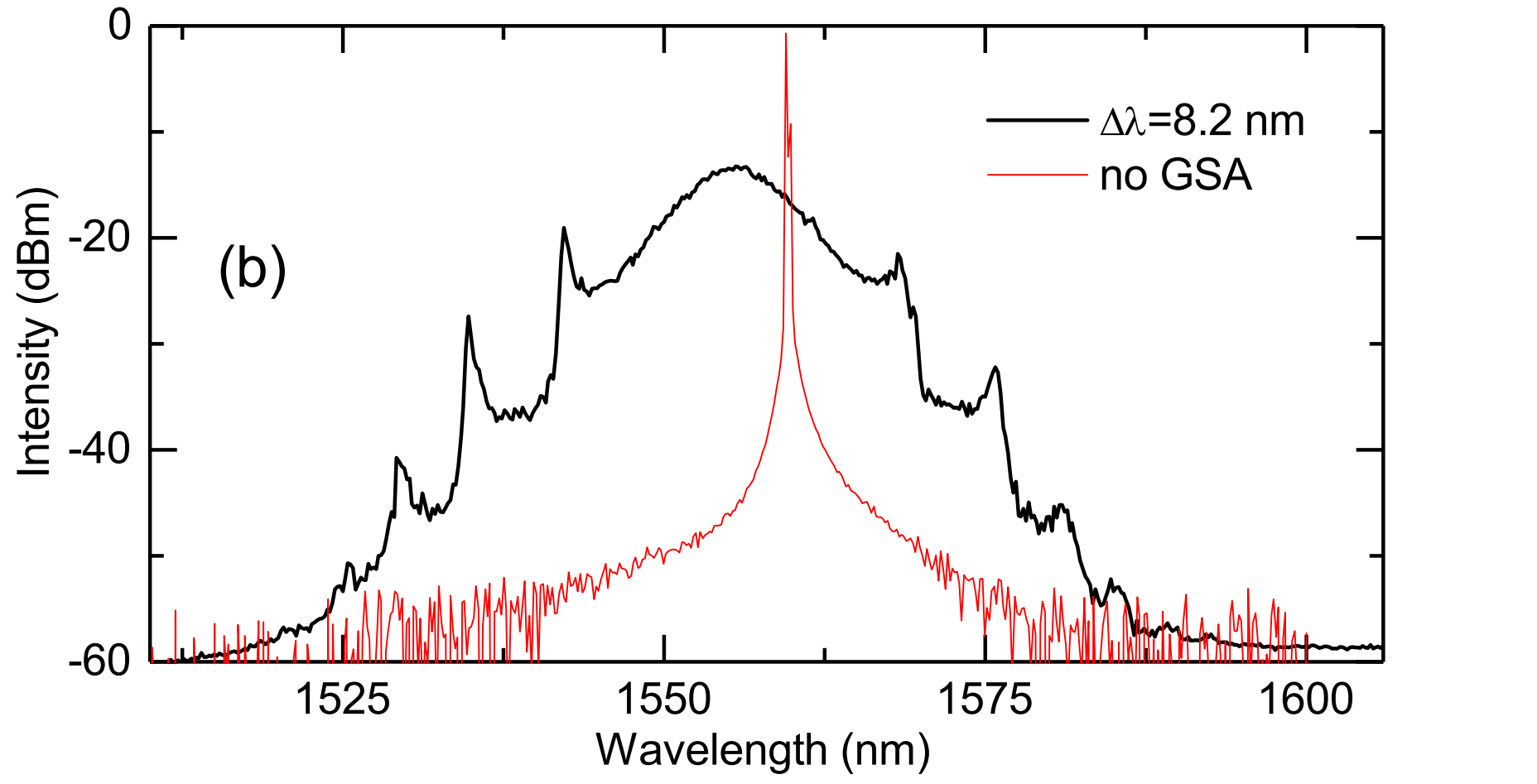
(b)
Intensity (dBm)
Wavelength (nm)
Δλ=8.2 nm
no GSA
0
-20
-40
-60
1525
1550
1575
1600

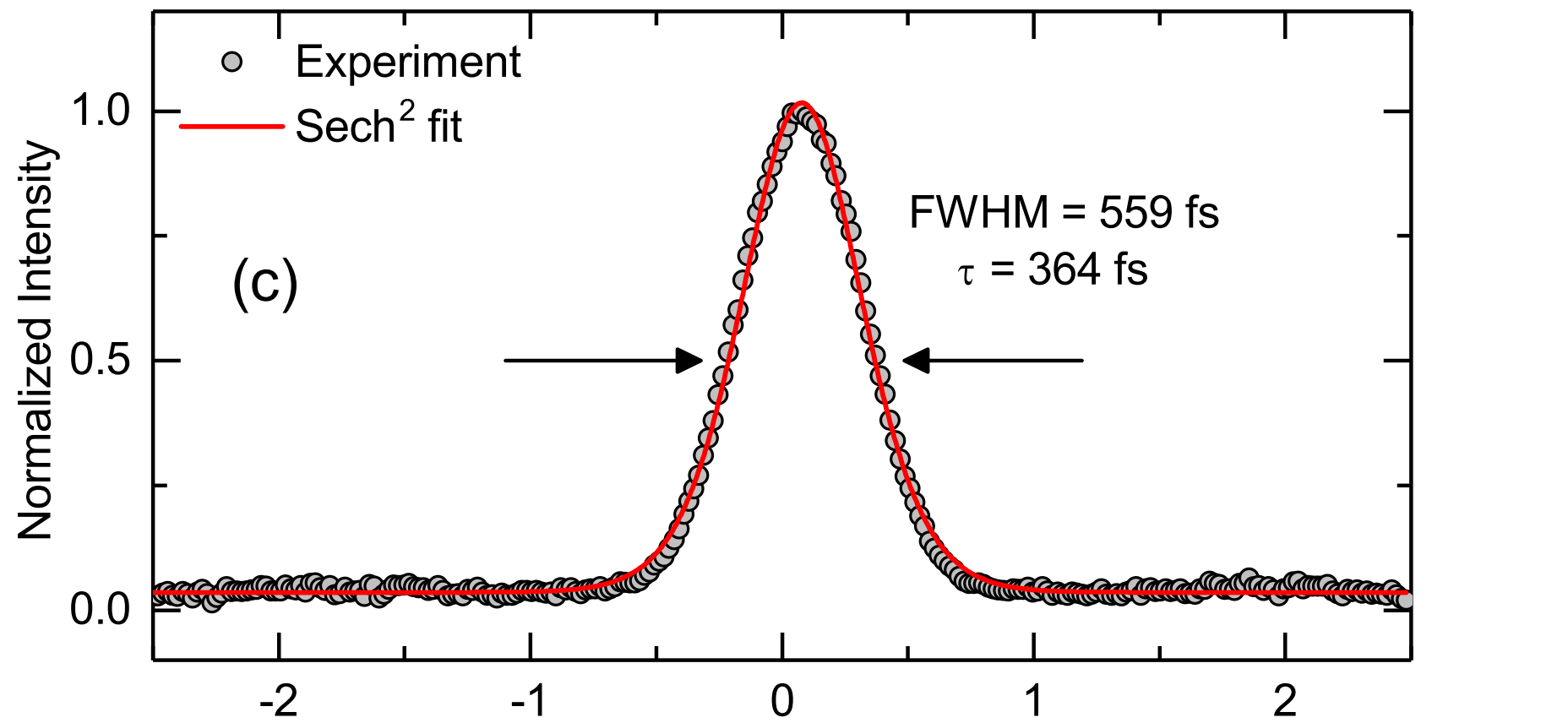
(c)
Normalized Intensity
Time (ps)
Experiment
Sech² fit
FWHM = 559 fs
τ = 364 fs
1.0
0.5
0.0
-2
-1
0
1
2

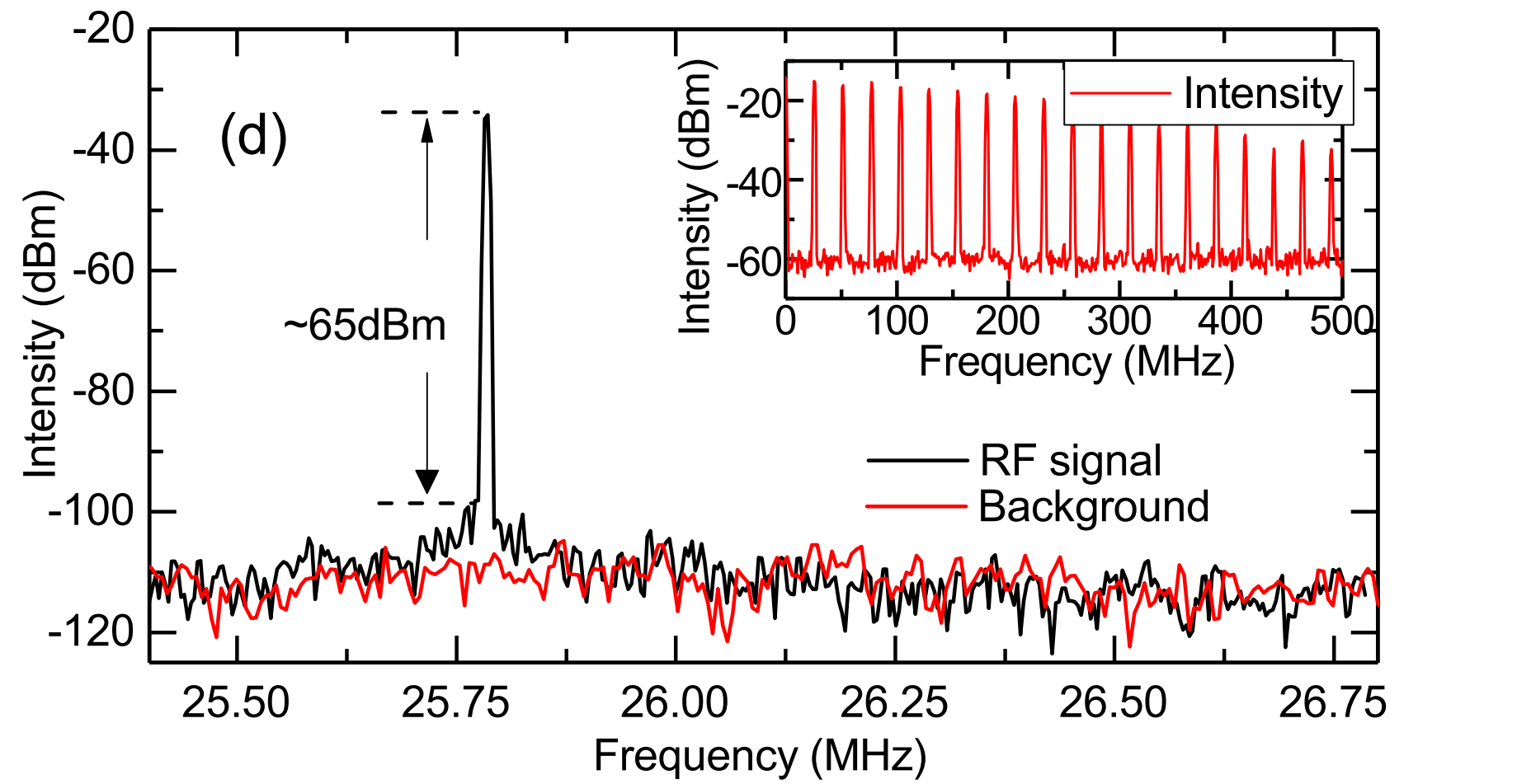
(d)
Intensity (dBm)
Frequency (MHz)
~65dBm
RF signal
Background
Intensity
-20
-40
-60
-80
-100
-120
25.50
25.75
26.00
26.25
26.50
26.75
0
100
200
300
400
500